Doniach Diagram of Disordered Electron Systems

Hyunyong Lee[1] and Stefan Kettemann[1, 2]

[1] *Division of Advanced Materials Science, Pohang University of Science and Technology (POSTECH), Pohang 790-784, South Korea**

[2] *School of Engineering and Science, Jacobs University Bremen, Bremen 28759, Germany*†

(Dated: November 9, 2012)

The quantum phase diagram of disordered electron systems (DES) with magnetic impurities (MIs) is derived. The competition between the indirect exchange interaction $|J_{\rm RKKY}|$ of magnetic impurities and the Kondo effect is known to give rise to a rich quantum phase diagram, the Doniach Diagram[1]. A Kondo screened phase is separated from a spin ordered phase at a quantum critical point (QCP), when the local exchange coupling J and the concentration of magnetic moments n are varied. We report here numerical results for disordered 2D electron systems which show that both the Kondo temperature T_K and $|J_{\rm RKKY}|$ are widely distributed and the QCP is extended to a critical region. Calculating the distribution function of their ratio $|J_{\rm RKKY}|/T_K$ for various separations R, we find a sharp cutoff, and from that a critical density $n_c(J)$. For lower densities that ratio is smaller than one for all sites, which we can identify therefore as the Kondo phase. As the disorder amplitude is increased, a phase of coupled magnetic moments (CM) grows at the expense of the Kondo phase. In addition, a paramagnetic (PM) phase where magnetic moments remain free at all temperatures arises below a critical exchange coupling J_c. Besides a low temperature Kondo Fermi liquid phase we find a phase with non-Fermi liquid behaviour with anomalous power law temperature dependence in the magnetic susceptibility and the specific heat. We confirm that these anomalous powers are related to the multifractality parameter α_0. The coupled moment phase shows a succession of 3 phases: a Griffiths phase with anomalous power laws determined by the distribution of $J_{\rm RKKY}$, a spin glass phase and a phase with long range magnetic order. We also report results on a honeycomb lattice, graphene, where we find that the magnetic phase is more stable against Kondo screening, but is more easily destroyed by disorder into a PM phase.

Phenomena which emerge from the interplay of strong correlations and disorder remain a challenge for condensed matter theory. Magnetic impurities (MIs) in metals are known to stir up the electronic Fermi liquid. These correlations result in a strong enhancement of the resistivity below the Kondo temperature T_K. Impurities are also known to result in Anderson localisation and lead to an exponential increase of resistivity at low electron densities. The interplay of Kondo effect with Anderson localisation has only recently received increased attention. However, spin correlations and disorder effects are relevant for many materials, including doped semiconductors like Si:P close to the metal-insulator transition[2], but also typical heavy Fermion systems, like materials with 4f or 5f atoms, notably Ce, Yb, or U[3, 4]. Many of these materials show a remarkable magnetic quantum phase transition which can be understood by the competition between indirect exchange interaction, the Ruderman-Kittel-Kasuya-Yoshida (RKKY) interaction between localised magnetic moments[5–7] and their Kondo screening. Thereby, one finds a suppression of long range magnetic order when the exchange coupling J is increased and Kondo screening succeeds. This results in a typical quantum phase diagram with a quantum critical point where the T_c of the magnetic phase is vanishing, the Doniach diagram[1]. In any material there is some degree of disorder. In doped semiconductors it arises from the random positioning of the dopants themselves, in heavy Fermion metals it may arise from structural defects or impurities. As noted already early[8], the physics of random systems is fully described by probability distributions, not just averages. This must be particularly true for systems with random local MIs[9]. In fact, it has been noticed that a wide distribution of T_K of MIs in disordered host metals gives rise to non-Fermi liquid behavior, such as the low temperature power-law divergence of the magnetic susceptibility[4, 9–16]. It was found[14, 17–20] that non-magnetic disorder quenches the Kondo screening of MIs due to Anderson-localisation and the formation of local pseudogaps at the Fermi energy. This results in bimodal distributions of T_K with a low T_K tail and a finite concentration of free, paramagnetic moments (PMs). From this distribution, the anomalous power law temperature dependence of the magnetic susceptibility and specific heat has been derived analytically and related directly to multifractality parameter α_0[19].

Accordingly, in order to be able to understand the magnetic properties of disordered magnetic systems, one needs to know also the distribution of the RKKY interaction $J_{\rm RKKY}$ between different MIs[5–7]. $J_{\rm RKKY}$ is mediated by the conduction electrons, and aligns the spins of the MIs ferromagnetically or antiferromagnetically, depending on their distance R. This is a long-ranged interaction, with a power law decay that is not changed by weak disorder[21–24]. It is known, that its amplitude has a wide log-normal distribution in disordered metals[21, 25]. Thus, to obtain the quantum phase diagram, the Doniach diagram of random systems with

MIs, we need to derive the full distribution functions of both T_K and $J_{\rm RKKY}$. This is the aim of this letter.

We present the results of numerical calculations, based on the kernel polynomial method, (KPM)[24, 26, 27] and compare them with previous analytical results, as obtained from the multifractal distribution of local intensities and their correlations[19]. We start from a microscopic description of the MIs, the Anderson impurity model coupled to a non-interacting disordered electronic Hamiltonian with on-site disorder. Then we map it with the Schrieffer-Wolff transformation on a model of Kondo impurities coupled to the disordered host electrons[19]. For the numerical calculations we employ the single-band Anderson tight-binding model on a square lattice of size L and lattice spacing a,

$$H = -t \sum_{\langle i,j \rangle} c_i^\dagger c_j + \sum_i (w_i - \varepsilon_F - \varepsilon_{\rm edge})\; c_i^\dagger c_i, \qquad (1)$$

where t is the hopping energy, c_i ($c_i^\dagger$) annihilates (creates) an electron at site i, w_i is the on-site random disorder energy distributed uniformly in the interval $[-W/2, W/2]$. $\langle i,j \rangle$ denotes the nearest-neighbor hopping, ε_F is the Fermi energy as measured from the band edge, $\varepsilon_{\rm edge} = -4t$ and periodic boundary conditions are used. We set Planck constant $\hbar$ and lattice spacing a to unity in the following.

We obtain T_K from the Nagaoka-Suhl equation [28]:

$$1 = \frac{J}{2} \int_0^D d\varepsilon \, \frac{\tanh[(\varepsilon - \varepsilon_F)/2T_K]}{\varepsilon - \varepsilon_F} \, \rho_{00}(\varepsilon), \qquad (2)$$

with band width D. The local density of states (LDOS) is defined by $\rho_{00}(\varepsilon) = \langle 0|\delta(\varepsilon - H)|0\rangle$. J is the local coupling constant between the localized MI and conduction electrons, ε_F is Fermi energy. The RKKY coupling $J_{\rm RKKY_{ij}}$ between two MIs located at positions $\boldsymbol{R}_i$, $\boldsymbol{R}_j$, is in the zero temperature limit ($T = 0$) given by[24–26]

$$J_{\rm RKKY_{ij}} = -J^2 \frac{S(S+1)}{2S^2} \int_{\varepsilon<\varepsilon_F} d\varepsilon \int_{\varepsilon'>\varepsilon_F} d\varepsilon' \frac{F(\varepsilon,\varepsilon')_{ij}}{\varepsilon - \varepsilon'}, \qquad (3)$$

where $F(\varepsilon,\varepsilon')_{ij} = {\rm Re}[\rho_{ij}(\varepsilon)\rho_{ji}(\varepsilon')]$, and S is the magnitude of the MI spin. Using the KPM, one can evaluate the matrix elements of the local density of states $\rho_{ij}(\varepsilon) = \langle i|\delta(\varepsilon - \hat{H})|j\rangle$[24, 27, 29, 30] with a Polynomial expansion of order M. In order to ensure convergence, but avoid finite size effects, we found that M should be increased linearly with system size L[25], for an explanation see Ref. [31]. Eq. (3) can be solved in a clean 2D system analytically[5], yielding $J^0_{\rm 2D} = -\frac{m^*}{8\pi} \sin(2k_F R)/(k_F R)^2$ in the asymptotic limit ($k_F R \gg 1$). $m^* = 1/(2a^2 t)$ is the effective electron mass, k_F the Fermi wave vector. A direct comparison between the exact analytical expression in the clean limit and the numerical result using the KPM method yields excellent agreement. In

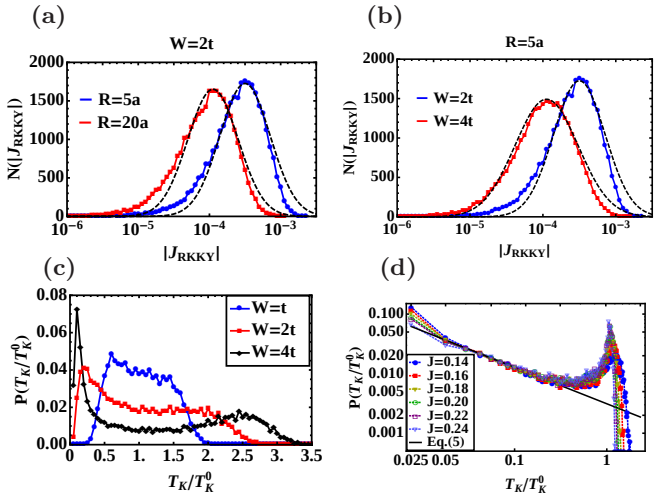

FIG. 1. (Color online) $N(J_{\rm RKKY})$ (a) for various distances R at $W = 2t$, (b) for various disorder W at $R = 5a$ ($N = 3000$, $L = 100a$, $M = 1000$). Black dashed lines: fit to log-normal distribution. (c) $P(T_K)$ for various disorder amplitudes W and $J/D = 0.25$, (d) $P(T_K)$ for $W = 5t$ and various $j = J/D$ (N=30 000, L=40a, M=200). $\varepsilon_F = 2t$ in a)-d).

accordance with Refs. 24 and 32, we find that the geometrical average amplitude of RKKY interaction decays exponentially for length scales exceeding localisation length ξ, $e^{\langle \frac{1}{2} \ln J^2_{\rm RKKY} \rangle} \sim e^{-R/\xi}$. In Figs. 1 a, b we show the distribution function of the absolute value of $J_{\rm RKKY}$ for various disorder amplitudes W and distances R. Black dashed lines are fitting curves based on the log-normal distribution, $P(x) = \frac{N}{\sqrt{2\pi}\sigma} \exp\left[-\frac{(x-x_0)^2}{2\sigma^2}\right]$, where $N = 3000$ is the total number of disorder configurations and $x = \ln|J_{\rm RKKY}|$. The fitting gives for $R = 5a$ and $W = 2t, 4t$ the parameter $x_0 = 5, 6$ and the width $\sigma = 5.3 + .85W/t$ increasing with the disorder strength W. We find that it does not depend strongly on the distance R, consistent with analytical results[21]. Next, we present in Fig. 1 c the distribution of T_K obtained from the numerical solution of Eq. (2) for $L = 40$, $j = 0.25$. For every sample only one single site is taken to avoid a distortion of the distribution due to intersite correlations. Therefore, we had to use a huge number of $N = 30\,000$ different random disorder configurations for each disorder amplitude W to get sufficient statistics. As found previously[13, 14, 33], the distribution has a strongly bimodal shape where the low T_K- peak becomes more distinctive with larger disorder amplitude W. In Fig. 1 d we compare these results with an analytical expression for the low T_K-tail of $P(T_K)$ in 2D DES, obtained in Ref. 19 from the multifractal distribution of intensities: In 2D DES there are weak wave function correlations which are logarithmic with an amplitude of order $1/g$. For weak disorder, $g \gg 1$, we can rewrite this correlation as an effective power law with power $\eta_{2D} = 2/\pi g$, where $g = \epsilon_F \tau$. The correlation energy in 2D is of the order

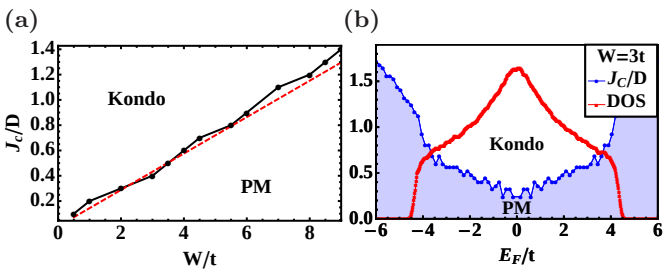

FIG. 2. (Color online) Critical exchange coupling J_c/D ($L = 100$) (a) as function of W ($M = 300, \varepsilon_F = 2t$). Red dashed line: Eq. (6). (b) as function of Fermi energy ($M = 200$). Red line: density of states (DOS).

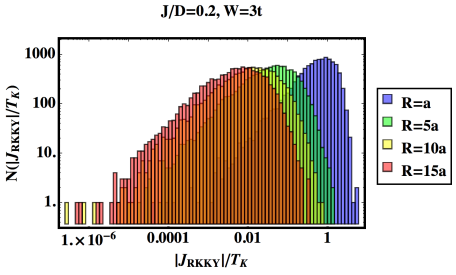

FIG. 3. (Color online) The probability of the ratio between the absolute value of RKKY interaction $|J_{\rm RKKY}|$ and Kondo temperature T_K for various distances R as indicated in the inset ($N = 3000, L = 100a, \varepsilon_F = t, M = 300$).

of the elastic scattering rate, $E_{c\,2D} \sim 1/\tau$. Thus, we find $P(T_K)$ for $T_K \ll \mathrm{Max}\{\Delta_\xi = D/\xi^2, \Delta = D/L^2\}$[19], where ξ is the localisation length and $D = 8t$,

$$P(T_K) = (1 - p_{FM}) \left(\frac{E_c}{T_K}\right)^{1-j} (\mathrm{Min}\{\xi, L\})^{-\frac{d^2 j^2}{2\eta_{2D}}}, \quad (4)$$

where $p_{FM} = n_{FM}(0)/n_M = (\mathrm{Min}\{\xi, L\})^{-\frac{d^2 j^2}{2\eta_{2D}}}$ is the ratio of free PMs, which has to be substracted from the weight of $P(T_K)$. We see that Eq. (4) has a power law tail with power $\beta_j = 1 - j$.

For $T_K^0 > T_K > \mathrm{Max}\{\Delta_\xi = D/\xi^2, \Delta = D/L^2\}$ we find that the power of the tail changes as [19]

$$\frac{P(T_K)}{1 - p_{FM}} = (\frac{E_c}{T_K})^{\frac{2d-\eta_{2D}}{2d}} \exp[-\frac{(\frac{T_K}{E_c})^{\frac{\eta_{2D}}{d}}}{2c_1} \ln^2 \left(\frac{T_K}{T_K^0}\right)] \quad (5)$$

where $c_1 = 7.51$. Here, ξ is the 2D localization length in absence of a magnetic field. For parabolic dispersion, valid for $0 < \epsilon_F - \epsilon_{\rm edge} \ll D$, one finds $\xi = g \exp(\pi g)$. The scattering rate $1/\tau$ is related to disorder amplitude W as $1/\tau = \pi W^2/6D$. In Fig. 1 d we compare with Eq. (5), using the analytical expression for η_{2D}, fitting $E_c \approx .13t$ and the prefactor. Thus, there is no dependence on j and the power depends only on η_{2D}. Only for the lowest $T_K \ll \Delta$, we find a deviation from Eq. (5), with a power law that increases with lowering j as $1 - j$ in good agreement with Eq. (4).

Next, we consider the quantum phase transition between the free paramagnetic moment phase (PM) and a Kondo phase[17]. We calculate the critical exchange coupling J_c above which there is no more than one free PM in the sample volume L^d. From the multifractality of the eigenfunction intensities we have found that J_c is related to the power η_{2D} of the power law correlations in the 2D DES as $J_c = \sqrt{\eta_{2D}} D$. Thus, we find that J_c increases in 2D linearly with disorder strength W as[19],

$$J_c = \sqrt{\frac{D}{3\varepsilon_F}} W. \quad (6)$$

In Fig. 2 a, we present the numerical results together with Eq. (6) as function of disorder strength W and find good agreement, with expected deviations at large disorder $g < 1$, where the $1/g$ expansion breaks down. According to Eq. (6) J_c increases as ε_F is moved towards the band edge. We have evaluated J_c for all ε_F and present the result along with density of states in Fig. 2 b. We find that J_c is increasing towards the band edge as $1/\sqrt{\varepsilon_F}$ in agreement with Eq. (6). Far outside of $\varepsilon_{\rm edge}$ of the clean system, it increases as expected with a gap in the DOS, as $J_c/D = 1/\ln|\varepsilon_{\rm edge} - \varepsilon_F|$.

Doniach Phase Diagram. In clean systems the critical density $n_c = 1/R_c^d$ above which the MIs are coupled with each other is obtained from the condition that $|J^0_{\rm RKKY}(R_c)| = T_K$. This yields in 2D with $|J^0_{\rm RKKY}|_{k_F R \gg 1} = J^2 \frac{m}{8\pi^2 k_F^2 R^2}$ and $T_K = c\varepsilon_F \exp(-D/J)$, $c \approx 1.14$ that $n_c = 16\pi^2 c \frac{\varepsilon_F^2}{J^2} \exp(-\frac{D}{J})$. In disordered systems, T_K at a certain site competes with the RKKY coupling with another MI at a distance R. Thus, we need to consider the distribution function of the ratio of these two energy scales $x_{JK} = |J_{\rm RKKY}(R)|/T_K$ for a given disordered sample with density of MIs $n = \frac{1}{R^2}$, where R is the average distance between the MIs. The distribution of x_{JK} for $W = 3t$ and $J/D = 0.2$ is shown for several R in Fig. 3. We see that it drops sharply at large values of x_{JK}, allowing us to define a critical density $n_c(J) = 1/R_c^2$ below which the Kondo effect dominates in the competition with RKKY interaction at all sites, see Fig. 4 a. This Kondo phase is split at finite temperature into a *Kondo Fermi-liquid (FL) phase*, where all MIs are screened, and for $T > T^*(J)$ a *Kondo Non-Fermi-liquid (NFL) phase* where some MIs remain unscreened and contribute to the magnetic susceptibility with an anomalous temperature dependence, given by[19],

$$\chi(T) \sim \frac{n_M}{E_c} \begin{cases} \frac{2d}{\eta} \left(\frac{T}{E_c}\right)^{\frac{\eta}{2d}-1} \text{for} & T > \frac{D}{\xi^2} \\ \frac{1}{j} \left(\frac{T}{E_c}\right)^{j-1} \xi^{-\frac{1}{2\eta}(dj)^2} \text{for} & T < \frac{D}{\xi^2} \end{cases} . \quad (7)$$

Here, $\eta = 2(\alpha_0 - d)$ depends for $d > 2$ on the universal multifractality parameter α_0. In $d = 2$ it is a function of W, $\eta_{2D}(W) = 2/\pi g(W)$. The temperature $T^*(n)$, see Fig. 4 c (blue line), is given by the position of the low T_K

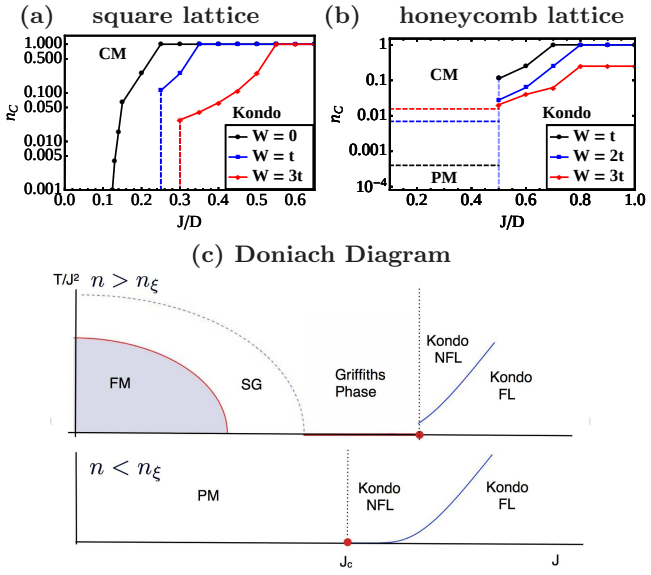

FIG. 4. (Color online) Critical MI density n_c as function of J/D for (a) square lattice ($\varepsilon_F = t$), (b) graphene ($\varepsilon_F = 3t$, Dirac point). L, M, N as in Fig. 3. For $n > n_c$ MIs are coupled (CM). (c) Schematic Doniach diagram: temperature T divided by J^2 versus J/D. Red dot, vertical dashed line: critical point $J_c(n)$ separating Griffiths phase from Kondo phase. Blue line: $T^*(n)$ separating Kondo FL phase from Kondo NFL phase. For $n < n_\xi$ and $J < J_c$ a paramagnetic phase (PM) appears.

peak in $P(T_K)$, see Fig. 1 c.

When the MI density n exceeds n_c, magnetic clusters start to form at some sites and the MIs may be coupled by $J_{\rm RKKY}(R)$. When R is larger than localisation length ξ the coupling $J_{\rm RKKY}(R)$ is exponentially small and there is a *paramagnetic phase* (PM) below $n_\xi = 1/\xi(g)^2$, where MIs remain free up to exponentially small temperatures. For $n > n_c$ there is a succession of phases, starting with the *Griffiths phase* where clusters are formed locally and anomalous power laws are observed when the clusters are broken up successively as temperature is raised. From the log-normal distribution $N(J_{RKKY})$ one obtains for the magnetic susceptibility, $\chi(T)T = n_{FM}(T) = \int_0^T dJ_{RKKY} N(J_{RKKY}) \sim n_M \exp[-\ln^2(T/J^0_{RKKY})/(2\sigma(W))^2]$, where the width $\sigma(W)$ depends on disorder strength W. Accordingly, the excess specific heat is $C(T) = T\frac{dn_{FM}}{dT} \sim \exp[-\ln^2(T/J^0_{RKKY})/(2\sigma(W)^2]$. At higher concentrations $n > n_{SG}$ a *spin-glass phase* appears, where the magnetic susceptibility shows a peak at spin glass temperature T_{SG} as studied in Refs. [34, 35]. Above a critical density n_F a phase with long range order may form[35–38]. In graphene the pseudogap at the Dirac point quenches the Kondo effect below $J_c = D/2$, independently on disorder W. Thus, there is a larger parameter space where the MIs are coupled (CM), see Fig. 4 (b). However, short range disorder localises the electrons, cutting off the RKKY-interaction and for $n < n_\xi$ there is a PM phase. Thus, we conclude that in graphene the magnetic phase is more stable against Kondo screening but is more easily destroyed by disorder.

We gratefully acknowledge useful discussions with Georges Bouzerar, Ki-Seok Kim, Eduardo Mucciolo and Keith Slevin. This research was supported by WCU (World Class University) program through the National Research Foundation of Korea funded by the Ministry of Education, Science and Technology(R31-2008-000-10059-0), Division of Advanced Materials Science.

* hyunyongrhee@postech.edu
† s.kettemann@jacobs-university.de

[1] S. Doniach, Physica B+C **91**, 231 (1977), ISSN 0378-4363.
[2] H. v. Löhneysen (Springer Berlin Heidelberg, 2000), vol. 40 of *Advances in Solid State Physics*, pp. 143–167, ISBN 978-3-540-41576-3.
[3] H. v. Löhneysen, A. Rosch, M. Vojta, and P. Wölfle, Rev. Mod. Phys. **79**, 1015 (2007).
[4] E. Miranda and V. Dobrosavljević, Reports on Progress in Physics **68**, 2337 (2005).
[5] M. A. Ruderman and C. Kittel, Phys. Rev. **96**, 99 (1954).
[6] T. Kasuya, Progress of Theoretical Physics **16**, 45 (1956).
[7] K. Yosida, Phys. Rev. **106**, 893 (1957).
[8] P. W. Anderson, Nobel Lectures in Physics **1980**, 376 (1977).
[9] Mott, N. F., J. Phys. Colloques **37**, C4 (1976).
[10] E. Miranda, G. Kotliar, and V. Dobrosavljević, Journal of Physics: Condensed Matter **8**, 9871 (1996).
[11] R. N. Bhatt and D. S. Fisher, Phys. Rev. Lett. **68**, 3072 (1992).
[12] A. Langenfeld and P. Wölfle, Annalen der Physik **507**, 43 (1995), ISSN 1521-3889.
[13] P. S. Cornaglia, D. R. Grempel, and C. A. Balseiro, Phys. Rev. Lett. **96**, 117209 (2006).
[14] S. Kettemann and E. R. Mucciolo, Phys. Rev. B **75**, 184407 (2007).
[15] A. H. Castro Neto, G. Castilla, and B. A. Jones, Phys. Rev. Lett. **81**, 3531 (1998).
[16] M. Sasaki, A. Ohnishi, T. Kikuchi, M. Kitaura, K.-S. Kim, and H.-J. Kim, Phys. Rev. B **82**, 224416 (2010).
[17] A. Zhuravlev, I. Zharekeshev, E. Gorelov, A. I. Lichtenstein, E. R. Mucciolo, and S. Kettemann, Phys. Rev. Lett. **99**, 247202 (2007).
[18] S. Kettemann and M. E. Raikh, Phys. Rev. Lett. **90**, 146601 (2003).
[19] S. Kettemann, E. R. Mucciolo, I. Varga, and K. Slevin, Phys. Rev. B **85**, 115112 (2012).
[20] S. Kettemann, E. R. Mucciolo, and I. Varga, Phys. Rev. Lett. **103**, 126401 (2009).
[21] I. V. Lerner, Phys. Rev. B **48**, 9462 (1993).
[22] L. N. Bulaevskii and S. V. Panyukov, JETP Lett. **43**, 240 (1986).
[23] G. Bergmann, Phys. Rev. B **36**, 2469 (1987).
[24] H. Lee, J. Kim, E. R. Mucciolo, G. Bouzerar, and S. Kettemann, Phys. Rev. B **85**, 075420 (2012).
[25] H. Lee, E. R. Mucciolo, G. Bouzerar, and S. Kettemann,

unpublished (2012).
[26] S. Roche and D. Mayou, Phys. Rev. B **60**, 322 (1999).
[27] A. Weiße, G. Wellein, A. Alvermann, and H. Fehske, Rev. Mod. Phys. **78**, 275 (2006).
[28] Y. Nagaoka, Phys. Rev. **138**, A1112 (1965).
[29] E. R. Mucciolo, unpublished (2010).
[30] H. Lee, E. R. Mucciolo, G. Bouzerar, and S. Kettemann, International Journal of Modern Physics: Conference Series **11**, 177 (2012).
[31] P. Wenk and G. Bouzerar, unpublished (2012).
[32] J. A. Sobota, D. Tanasković, and V. Dobrosavljević, Phys. Rev. B **76**, 245106 (2007).
[33] S. Kettemann and E. Mucciolo, JETP Letters **83**, 240 (2006), ISSN 0021-3640, 10.1134/S0021364006060051.
[34] K. Binder and A. P. Young, Rev. Mod. Phys. **58**, 801 (1986).
[35] B. Coqblin, C. Lacroix, M. A. Gusmão, and J. R. Iglesias, Phys. Rev. B **67**, 064417 (2003).
[36] C. M. Varma, Rev. Mod. Phys. **48**, 219 (1976).
[37] S. G. Magalhaes, F. M. Zimmer, P. R. Krebs, and B. Coqblin, Phys. Rev. B **74**, 014427 (2006).
[38] G. Bouzerar and T. Ziman, Phys. Rev. Lett. **96**, 207602 (2006).